An analytical prediction of the oscillation and extinction thresholds of a clarinet

Jean-Pierre Dalmont[a] and Joël Gilbert
Laboratoire d'Acoustique de l'Université du Maine (UMR CNRS 6613), Université du Maine, 72085, Le Mans, France

Jean Kergomard
Laboratoire de Mecanique et d'Acoustique (UPR CNRS 7051), 31 Ch. Joseph Aiguier, 13402, Marseille, France

Sébastien Ollivier[b]
Laboratoire d'Acoustique de l'Université du Maine (UMR CNRS 6613), Université du Maine, 72085, Le Mans, France

(Received 24 January 2005; revised 25 July 2005; accepted 25 July 2005)

This paper investigates the dynamic range of the clarinet from the oscillation threshold to the extinction at high pressure level. The use of an elementary model for the reed-mouthpiece valve effect combined with a simplified model of the pipe assuming frequency independent losses (Raman's model) allows an analytical calculation of the oscillations and their stability analysis. The different thresholds are shown to depend on parameters related to embouchure parameters and to the absorption coefficient in the pipe. Their values determine the dynamic range of the fundamental oscillations and the bifurcation scheme at the extinction. © *2005 Acoustical Society of America.* [DOI: 10.1121/1.2041207]

PACS number(s): 43.75.Pq [NHF] Pages: 3294–3305

I. INTRODUCTION

When a clarinet is blown with an increasing mouth pressure, for a fixed embouchure, the reed begins to oscillate for a particular pressure value, called "threshold of oscillation," and stops at another value, called here "threshold of extinction." Above this threshold the reed is held motionless against the lay. These two thresholds determine the dynamic range of the clarinet for given embouchure parameters. The threshold of oscillation has been extensively studied in the literature (see, e.g., Grand *et al.*, 1997; Kergomard *et al.*, 2000). On the contrary, the threshold of extinction has been only recently investigated (Dalmont *et al.*, 2002; Atig *et al.*, 2004) despite being of crucial importance in the playing of the clarinet. Experiments have shown that the threshold of extinction above which the oscillations stop is larger than the minimum mouth pressure p_M sufficient to maintain the reed channel closed (Dalmont *et al.*, 2000). It has also been observed that losses in the pipe and especially nonlinear losses at side holes might influence significantly the value of the extinction threshold, that is, consequently, the maximum power of a given instrument (Atig *et al.*, 2004).

The aim of the present paper is to investigate the playing range of the clarinet for the fundamental regime (first register) and to bring out the physical parameters which determine this range. To allow an analytical study, this analysis is based on a simplified model of the clarinet. The simplest model is to consider the body of the clarinet as an open straight pipe without any radiation or thermoviscous losses. This model is called here "lossless model" and has been extensively studied by Kergomard (1995) and Maganza *et al.* (1986) for example. However, it is not able to describe the extinction phenomenon at high blowing pressures since with this model, unless a nonlinear effect is introduced, there is no limit to the amplitude of the acoustic pressure when the mouth pressure is increased. Experiments and simulations suggest that losses have to be introduced in the model Atig *et al.*, (2004). In order to allow analytical calculations, losses in the pipe are introduced by means of a constant parameter, independent of the frequency. This kind of model has been extensively used for the bowed string (Raman, 1918; Schelleng, 1973; Mc Intyre *et al.*1983;Woodhouse, 1993) and appears to be useful for the study of reed woodwinds oscillations (Ollivier *et al.*, 2004, 2005), therefore it is referred to in the following as "Raman's model." In the present paper, it is shown to be sufficiently simple to allow analytical calculations, in particular of the different threshold values.

In an extended state of the art (Sec. II) the model is presented (Sec. II A) and the results for the static solution and small oscillations are reviewed (Sec. II B), as well as results obtained with a lossless model (Sec. II C). Raman's model is used to calculate the periodic solutions at the fundamental frequency from which bifurcation diagrams are derived (Sec. III). Some thresholds are calculated (Sec. III C) and stability of the periodic solutions giving the bifurcation schemes is discussed in Sec. III D. For clarity the details of calculations are given in Appendix A. Some consequences about the playing range of the musical instrument are discussed in Sec. IV.

[a]Author to whom correspondence should be addressed; electronic mail: jean-pierre.dalmont@univ-lemans.fr
[b]Present affiliation: Laboratoire de Mécanique des Fluides et d'Acoustique (UMR CNRS 5509) Ecole Centrale de Lyon, Ecully, France.

II. STATE OF THE ART

A. Equations of the model

The clarinet can be divided into two parts, each being described by a single equation: one is the body of the instrument (the pipe) and one is the reed-mouthpiece set (the generator).

1. The pipe

The pipe of the clarinet is assumed to be perfectly cylindrical. The lowest level of approximation is given by the lossless approximation in which a total reflection at the end of the pipe is assumed and losses in the pipe are ignored. The corresponding reflection function for pressure $r(t)$ at the input is given by

$$r(t) = -\delta(t-\tau), \tag{1}$$

where the delta function $\delta(t)$ is delayed by $\tau = 2L/c$, that is the roundtrip travel time of a wave at speed c along the pipe of length L.

A higher level of modeling might take into account the visco-thermal dissipation and dispersion effect (see, for example, Polack *et al.*, 1987) as well as the radiation impedance (Norris and Sheng, 1989; Nederveen, 1998; Dalmont *et al.*, 2001b). An intermediate level is the so-called "Raman's model," ignoring dispersion and assuming that losses, including radiation, are frequency independent. The reflection function $r(t)$ is then given by

$$r(t) = -e^{-2\alpha L}\delta(t-\tau), \tag{2}$$

where the constant parameter α is the absorption coefficient. In the frequency domain, the Fourier transform of the reflection function is the reflection coefficient:

$$R(\omega) = -e^{-2j(k-j\alpha)L}, \tag{3}$$

where $k = \omega/c$ is the wavenumber.

The input impedance of the pipe $Z = p/u$, where p and u are the acoustic pressure and volume velocity, respectively, can be obtained from the reflection coefficient

$$Z(\omega) = Z_c \frac{1+R(\omega)}{1-R(\omega)} = jZ_c \tan[(k-j\alpha)L], \tag{4}$$

where $Z_c \approx \rho c/S$ is the characteristic impedance of the pipe, S being the cross-section area and ρ the density of air. In practice, the absorption coefficient $\alpha(f)$ is frequency dependent and is given, for a straight pipe, by

$$\alpha(f) \approx 3 \cdot 10^{-5}\sqrt{f}/a, \tag{5}$$

where f is the frequency in Hz and a the radius of the pipe expressed in MKS units [see, e.g., Fletcher and Rossing (1998), p. 196]. In the present paper, the value of α is calculated at the first resonant frequency, that is for $f = c/4L$, and as α is assumed to be independent of the frequency, all the resonance peaks have the same amplitude (Fig. 1), the admittance at resonance $f_n = (2n-1)c/4L$ being real and equal to

$$Y = 1/Z = \tanh(\alpha L)/Z_c. \tag{6}$$

At zero frequency the input impedance is given by

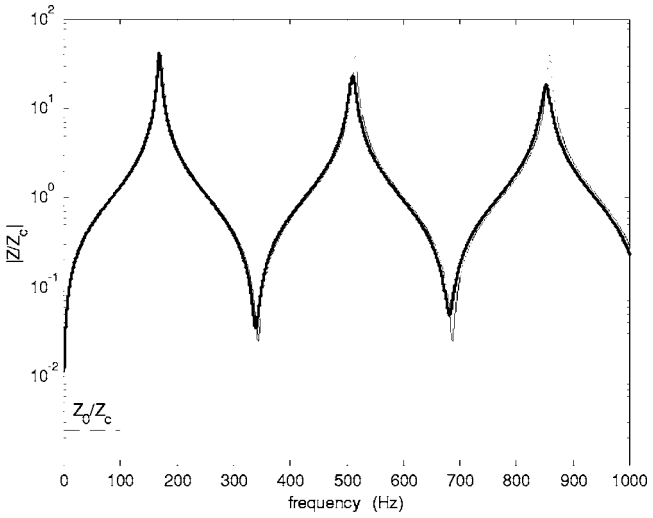

FIG. 1. Reduced input impedance Z/Z_c of an open cylinder of 50 cm length and 8 mm radius. Thick line: model with viscothermal losses. Thin line: Raman's model without dispersion and with frequency independent losses. The horizontal dotted line indicates the limit value of the impedance when frequency tends toward zero according to a Poiseuille flow.

$$Z_0 = Z_c \tanh(\alpha L). \tag{7}$$

This value is probably much larger than the real value because the value of α is not valid for $f = 0$. The input impedance Z_0 could be calculated for example by using the Poiseuille equation for viscous laminar flow which leads to a much lower value [Reynolds number is shown to be lower than 500 in Kergomard (1995), p. 250]: for a 16-mm-diam pipe of length 0.5 m, $\alpha L = 0.025$ at first resonant frequency and should be $\alpha_0 L = 0.001\,25$ at zero frequency according to Poiseuille equation.

2. The generator

The second part of the system, the reed mouthpiece set, acts as a valve [see, for example, Wilson and Beavers (1974) or Hirschberg (1995)]. The volume velocity $u(t)$ through the reed slit is controlled by the aperture height $H(t)$ between the reed and the mouthpiece, and by the velocity of the air $v(t)$. This velocity depends nonlinearly on the pressure difference Δp equal to the mouth pressure p_m, assumed to be static, minus the acoustic pressure $p(t)$ in the mouthpiece (see Fig. 2)

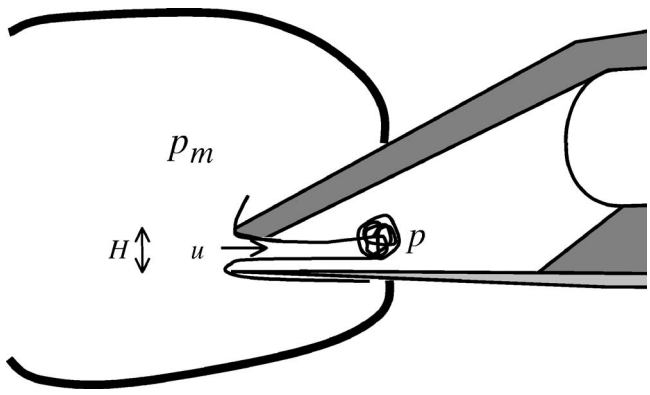

FIG. 2. Schematic view of the mouthpiece.

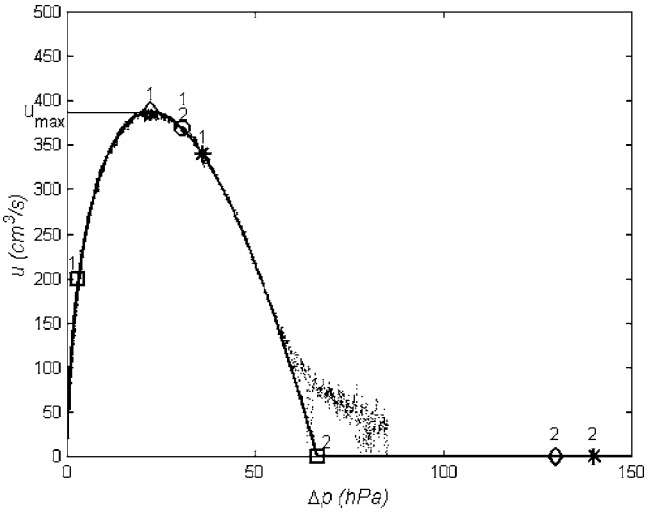

FIG. 3. Nonlinear characteristics: flow through the reed channel vs the pressure difference on both sides of the reed. Thick line: model; thin line: experiment (adapted from Dalmont *et al.*, 2003; experiment stops at $\Delta p = 85$ hPa). The points $(\Delta p_1, u_1)$ and $(\Delta p_2, u_2)$ corresponding to the different thresholds are labeled on the curve: (○) threshold of oscillation ($\Delta p_1 = \Delta p_2$); (□) beating reed threshold; (◇) saturation threshold; (∗) extinction threshold.

$$\Delta p(t) = p_m - p(t). \tag{8}$$

The nonlinear equation comes from Bernoulli equation and is based on the assumption that the kinetic energy of the jet entering in the instrument is completely dissipated into turbulence during its expansion into the mouthpiece:

$$v(t) = \sqrt{\frac{2\Delta p(t)}{\rho}}. \tag{9}$$

The volume velocity $u(t)$ is proportional to the jet cross section $S_{\text{jet}}(t)$, and is given by

$$u(t) = S_{\text{jet}}(t)v(t). \tag{10}$$

The cross section of the jet is assumed to be equal to the reed slit opening surface which is assumed to be rectangular and proportional to the height of the opening $H(t)$:

$$S_{\text{jet}}(t) = wH(t), \tag{11}$$

where w is the effective width of the slit [see Dalmont *et al.* (2003) for a detailed discussion]. The reed is assumed to behave as an ideal spring characterized by its stiffness K (in Pa/m). Then $H(t)$ is linearly dependent on the pressure difference $\Delta p(t)$:

$$H(t) = H_0\left(1 - \frac{\Delta p(t)}{p_M}\right) \quad \text{if } \Delta p(t) \leqslant p_M$$

$$H(t) = 0 \quad \text{if } \Delta p(t) \geqslant p_M, \tag{12}$$

where H_0 is the opening at rest and $p_M = KH_0$ is the lowest pressure for which the reed channel is closed, the reed being held against the lay in static regime.

Combining Eqs. (8)–(12) leads to an instantaneous relationship between the volume velocity $u(t)$ and the pressure difference $\Delta p(t)$:

TABLE I. Typical range values of the embouchure parameters.

w (mm)	p_m (hPa)	H_0 (mm)	K (hPa/mm)	p_M (hPa)	u_A (cm^3/s)
10–13	0–150	0.2–1.1	50–500	40–100	100–2000

$$u = F(p) = u_A\left(1 - \frac{\Delta p}{p_M}\right)\sqrt{\frac{\Delta p}{p_M}} \quad \text{if } \Delta p \leqslant p_M,$$

$$u = F(p) = 0 \quad \text{if } \Delta p \geqslant p_M, \tag{13}$$

where

$$u_A = wH_0\sqrt{\frac{2KH_0}{\rho}} \tag{14}$$

is a volume velocity amplitude parameter. This function $F(p)$ is the nonlinear characteristics of the embouchure. The parameter u_A is related to the maximum flow of the nonlinear characteristics $u_{\max}$ by

$$u_A = \frac{3\sqrt{3}}{2}u_{\max}.$$

Then the elementary model can be reduced to two equations, Eq. (13) characterizing the valve effect (reed) and Eq. (2) characterizing the resonator by its reflection function. Many assumptions behind this elementary model require further discussion (see Hirschberg, 1995), however, recent work has shown that this model fits rather well with the pressure flow characteristics measured in a real clarinet mouthpiece blown by using an artificial mouth setup [see Fig. 3 adapted from Dalmont *et al.* (2003)].

To summarize, seven parameters are involved in the physical model. Three are related to the pipe: the length L of the pipe, the absorption coefficient α, and the characteristic impedance of the pipe $Z_c = \rho c/S$ which depends on the cross section of the pipe. All three are fixed for a given length of the pipe. Four parameters are related to the embouchure: the effective width of the reed channel w, the reed slit opening at rest H_0, the reed stiffness K, and the mouth pressure p_m. The parameter w can be considered as almost constant. The mouth pressure p_m can be varied and controlled by the player as well as the embouchure parameters K and H_0. Typical values of the parameter ranges are given in Table I (see also Dalmont *et al.*, 2003).

B. Static solution and small oscillations for a lossy resonator

The static solution can be found from Eq. (13). This corresponds to the equilibrium state of the reed associated to each value of the mouth pressure p_m in the absence of sound. If losses at zero frequency are ignored ($Z_0 = 0$ and $p = 0$), the following values for the volume velocity u_{eq} and the aperture height H_{eq} are obtained:

$$u_{\text{eq}} = u_A\left(1 - \frac{p_m}{p_M}\right)\sqrt{\frac{p_m}{p_M}},$$

$$H_{\text{eq}} = H_0\left(1 - \frac{p_m}{p_M}\right). \tag{15}$$

The set of Eq. (15) is valid if $p_m < p_M$, otherwise the reed is held against the lay and then u_{eq} and H_{eq} are both equal to zero. The static solution is stable only for given values of the mouth pressure. Some papers have explored the equilibrium solution stability [for a review, see Fletcher and Rossing (1998)]. The main result is that the static solution is stable at low values of p_m, and becomes unstable from a particular value of mouth pressure, denoted $p_{m\text{th}}$. Applying the results of Grand *et al.* (1997) to the present model, it can be shown (Dalmont *et al.*, 2000) that a direct bifurcation is found regardless of the values of the control parameters. As a consequence, the threshold of instability of the static solution is also the threshold of oscillation. The threshold value $p_{m\text{th}}$ is reached for $\partial u/\partial p_m = -Y$ where Y is the value of the admittance at the first resonant frequency and given by Eq. (6). An elementary calculation gives the value of $\Delta p = p_m - p$ at the threshold of oscillation (Kergomard *et al.*, 2000),

$$\Delta p_{\text{th}} = \left(\frac{1}{3} + \frac{2}{3\sqrt{3}}\beta_1\sqrt{1 + \beta_1^2/3} + \frac{2\beta_1^2}{9}\right)p_M, \tag{16}$$

where

$$\beta_1 = Y\frac{p_M}{u_A} = \frac{p_M}{Z_c u_A}\tanh \alpha L. \tag{17}$$

It should be noted that Eq. (16) is obtained as well with Raman's model as with a more sophisticated model of the impedance of the pipe and despite the fact that Raman's model leads to a square signal rather than a sinusoidal one at the threshold of oscillation (see Kergomard *et al.*, 2000). In the absence of losses (i.e., $\alpha = 0$), Y is zero at the resonance, then β_1 is also equal to zero and the threshold of oscillation is found to be $p_{m\text{th}} = p_M/3$. When either losses are large or u_A/p_M (the flow parameter to closing pressure ratio) is small the threshold of oscillations tends to p_M when β_1 tends to unity. On the other hand, when the value of the mouth pressure is larger than p_M, the reed is held against the lay, and the static solution is stable again because $\partial u/\partial p_m$ and all the other derivatives are equal to zero. As a consequence since $p_{m\text{th}} > p_M$ the equilibrium state is always stable, no oscillation at all is possible. This situation is easy to obtain in practice: if the reed opening is too small no oscillation for any mouth pressure occurs despite the fact that the threshold value is finite.

C. Lossless model: Periodic solutions and stability analysis

The use of a lossless model for the resonator has been initiated independently by Friedlandler (1953) and Keller (1953) for the bowed string. This approximation cannot lead to stable periodic oscillations of the bowed string if combined with stick-slip characteristics which assume a perfect sticking of the bow on the string (Friedlander, 1953; Woodhouse, 1993). On the contrary, stable oscillations can be obtained with a lossless model of a reed instrument because of the "smoother" nonlinear characteristics plotted in Fig. 3 (Ollivier *et al.*, 2004, 2005). The use of a lossless model for the resonator cannot provide information on the evolution of the spectrum, but it is fruitful for the study of stability, transients, and bifurcations. This approach has been first used for the clarinet by Maganza (1986), who investigated period doubling mechanism. More recently Kergomard (1995) used such a model to analyze the role of the main control parameters on the oscillations of a clarinet. Lossless models have also been fruitfully applied to stepped cones [see, for example, Dalmont and Kergomard (1995) or Dalmont *et al.* (2000) for theoretical and experimental comparison].

Important results stemming from the lossless approximation and the method used to derive them are now recalled. Given the reflection function $r(t) = -\delta(t-\tau)$ [Eq. (1)], the positive and negative going plane wave pressures at the input (p^+ and p^-, respectively) are related by

$$p^-(t) = r(t)p^+(t) = -p^+(t-\tau). \tag{18}$$

The acoustical field is fully described by using the pair of variables $\{p^+, p^-\}$ or the pair $\{p, u\}$ which are related by

$$p(t) = p^+(t) + p^-(t),$$

$$Z_c u(t) = p^+(t) - p^-(t),$$

or

$$p^+(t) = \tfrac{1}{2}(p(t) + Z_c u(t)),$$

$$p^-(t) = \tfrac{1}{2}(p(t) - Z_c u(t)). \tag{19}$$

Using discrete-time representation, the acoustical field is calculated at every sampling period, by using the sampling frequency $f_s = 1/\tau = c/2L$ which is twice the fundamental resonant frequency of the pipe. In order to simplify the notations, $p(t)$ at $t = n\tau$ is written p_n, the nth sample. Then Eq. (18) is written as $p_n^- = -p_{n-1}^+$ or, using Eq. (19), as

$$p_n - Z_c u_n = -(p_{n-1} + Z_c u_{n-1}). \tag{20}$$

Searching for the periodic regimes of fundamental frequency $c/4L$, the periodicity of the solutions leads to $p_{n+1} = p_{n-1}$ and $u_{n+1} = u_{n-1}$. Applying Eq. (20) for two successive steps leads to

$$p_n = -p_{n-1},$$

$$u_n = u_{n-1}. \tag{21}$$

Using Eq. (21) and the nonlinear characteristics $u_n = F(p_n)$, the function $F(p)$ being given by Eq. (13) with $\Delta p_n = p_m - p_n$ (p_m is the mouth pressure), the solutions at the fundamental frequency can be obtained. An extensive study of the periodic solutions is done in Kergomard (1995). Two kinds of periodic regimes are distinguished: the nonbeating reed regime and the beating reed regime for which one of the two states of the reed is held motionless against the lay. The nonbeating reed regime occurs for $p_M/3 \leqslant p_m \leqslant p_M/2$. In that range of pressures it can be shown that $p_n = -p_{n-1} = \sqrt{(3p_m - p_M)(p_M - p_m)}$. The beating reed regime occurs for $p_m > p_M/2$ and it can be shown that in that case $p_n = -p_{n-1} = p_m$ and $u_n = u_{n-1} = 0$.

As explained by Kergomard (1995) or Ollivier *et al.* (2004, 2005) the periodic solutions are stable if the following inequality is true:

$$F_{\text{stab}}(p) < 0, \tag{22}$$

where

$$F_{\text{stab}}(p) = \frac{F'(p) + F'(-p)}{1 + Z_c^2 F'(p) F'(-p)} \tag{23}$$

is the stability function, F' being the first derivative of the nonlinear characteristic Eq. (13). A conclusion of the stability analysis is that the beating reed regime is always stable. The nonbeating reed regime is stable under certain control parameters conditions, that is:

$$Z_c^2 u_A^2 < \frac{2(p_M - 2p_m)p_M^3}{(3p_m - p_M)(5p_M - 6p_M)}. \tag{24}$$

For a fixed value of u_A, this condition is satisfied below a limit value of p_m. Above this limit, a range of mouth pressure is found for which the oscillation is not stable and in this range period doubling bifurcations can be found. Several regimes where periods are multiple of these of the fundamental frequency $f=c/4L$ can exist. For these regimes the reed can beat for mouth pressures lower than $p_M/2$ [see the curves for the volume velocity in Fig. 8, p. 253 of Kergomard (1995)]. So, the value $p_m=p_M/2$ which is called the beating reed threshold (for the lossless model) is the beating reed threshold only for the oscillating regime of fundamental frequency $f=c/4L$.

III. RAMAN'S MODEL: PERIODIC SOLUTIONS AND THEIR STABILITY

As discussed in Dalmont *et al.* (2002), the main weakness of the lossless model is that it allows periodic oscillations for every mouth pressure above the threshold of oscillation, showing no extinction phenomenon. Recently Atig *et al.* (2004) have shown theoretically and experimentally how losses can modify and control the saturation and extinction phenomena. The simplest way to take into account losses in a theoretical approach is to use a Raman's model in which losses are independent of the frequency and in which the dispersion phenomenon is ignored. This model, and its dynamic behavior (oscillating solutions, bifurcation diagrams) is described in the following.

A. Equations of Raman's model

Taking into account a frequency independent absorption coefficient α, and using Eq. (2), Eq. (18) becomes

$$p^-(t) = r(t)^* p^+(t) = -e^{-2\alpha L} p^+(t-\tau). \tag{25}$$

In the discrete-time representation, Eq. (20) becomes

$$p_n - Z_c u_n = -e^{-2\alpha L}(p_{n-1} + Z_c u_{n-1}). \tag{26}$$

The instantaneous relationship defining the volume velocity u [Eq. (13)] remains valid. The slight complication introduced in Eq. (26) as compared to Eq. (20) implies that Eq. (21) is no longer valid. The periodic solutions of the Raman's model cannot be derived so easily. This difficulty is overcome by a change in variables, where a new pair of variables, $\{q,w\}$, is defined as a function of the pair $\{p,u\}$, as follows:

$$q = p\cosh(\alpha L) - Z_c u \sinh(\alpha L),$$

$$w = Z_c u \cosh(\alpha L) - p \sinh(\alpha L). \tag{27}$$

The left and the right traveling pressure waves in the open end of the pipe (p_o^+ and p_o^-, respectively) can be successively written as functions of the pair $\{p,u\}$, and as functions of the pair of variables $\{q,w\}$:

$$\begin{aligned} p_o^+ &= e^{-\alpha L} p_{n-1}^+ = e^{-\alpha L}\tfrac{1}{2}(p_{n-1} + Z_c u_{n-1}) \\ &= (\cosh \alpha L - \sinh \alpha L)\tfrac{1}{2}(p_{n-1} + Z_c u_{n-1}) \\ &= \tfrac{1}{2}(q_{n-1} + w_{n-1}), \end{aligned}$$

$$\begin{aligned} p_o^-(t) &= e^{+\alpha L} p_n^- = e^{+\alpha L}\tfrac{1}{2}(p_n - Z_c u) \\ &= (\cosh \alpha L + \sinh \alpha L)\tfrac{1}{2}(p_{n-1} + Z_c u_{n-1}) \\ &= \tfrac{1}{2}(q_n - w_n). \end{aligned} \tag{28}$$

With this change of variables the problem is formally similar to that for the lossless model. Results are identical except that the instantaneous relationship defining the volume velocity u as a function of p Eq. (13) must be transformed into a new relationship between w and q:

$$w_n = G(q_n). \tag{29}$$

Function G is known only implicitly since an explicit expression is difficult to find. Nevertheless an expression of its derivative can be obtained, as shown in Sec. III D. Assuming that at the open end the boundary condition is a pressure node [Eq. (18)], Eq. (28) leads to

$$q_n - w_n = -(q_{n-1} + w_{n-1}). \tag{30}$$

The acoustical field can be calculated step by step in time, by using Eqs. (29) and (30) where the unknowns are q and w. These equations are formally identical to Eqs. (13) and (20) where the unknowns are p and u. Then searching for the periodic regimes, that is determining the two states of the periodic solution, leads to solve the following set of equations, similar to Eq. (21):

$$q_n = -q_{n-1},$$

$$w_n = w_{n-1}. \tag{31}$$

Similar to the lossless model results [Eqs. (22) and (23)], the periodic solutions are stable if the following inequality is true:

$$G_{\text{stab}}(q) < 0, \tag{32}$$

where

$$G_{\text{stab}}(q) = \frac{G'(q) + G'(-q)}{1 + G'(q)G'(-q)} \tag{33}$$

is the stability function, G' being the first derivative of G.

B. Periodic solutions and bifurcation diagrams

The periodic regimes are defined by the two different values of the acoustic pressure corresponding to the two alternate states of the reed position. Let p_1 and p_2 be the pressure in the mouthpiece for two successive states and u_1 and u_2 the corresponding volume velocities. These two pressures are solutions of Eq. (26), which, using Eqs. (6) and (7), leads to

$$p_1 + p_2 = (Z_c u_1 + Z_c u_2)\tanh\,\alpha L = Z_0(u_1 + u_2),$$

$$u_1 - u_2 = (p_1 - p_2)\tanh\,\alpha L/Z_c = Y(p_1 - p_2). \tag{34}$$

The first equation expresses that the ratio of mean value of the pressure to the mean value of the volume velocity is equal to the impedance at zero frequency. At this stage it is reasonable to consider that this impedance is low, that is to assume $p_1 \approx -p_2$. The second equation expresses that the ratio of the pressure difference to the volume velocity difference is equal to the impedance at the resonant frequencies. It is convenient, for the calculations of the solutions, to define the following dimensionless parameters:

$$\beta = Z_0\frac{u_A}{p_M} = \frac{Z_c u_A}{p_M}\tanh\,\alpha L,$$

$$\beta_1 = Y\frac{p_M}{u_A} = \frac{p_M}{Z_c u_A}\tanh\,\alpha L,$$

$$\beta_2 = \frac{2\beta_1}{1+\beta\beta_1} = \frac{p_M}{Z_c u_A}\tanh\,2\alpha L. \tag{35}$$

The first one, β, can be seen as the adimensioned impedance at zero frequency and the second, β_1, as the adimensioned admittance at playing frequency. The parameter β_2 is a combination of the two others and it can be noted that, if $\alpha L \ll 1$, which is usually the case, $\beta \approx 0$ and $\beta_2 \approx 2\beta_1$.

1. Beating reed regime

The beating reed regime is attained for $\Delta p = p_m - p \geqslant p_M$. So, the set of equations (34) is simplified by the fact that $u_2 = 0$, state 2 being arbitrarily considered as the closed state. Then it follows from Eq. (34):

$$p_1 + p_2 = Z_c u_1 \tanh\,\alpha L,$$

$$Z_c u_1 = (p_1 - p_2)\tanh\,\alpha L, \tag{36}$$

which implies

$$p_2 = p_1\frac{(\tanh^2\,\alpha L - 1)}{(\tanh^2\,\alpha L + 1)}$$

$$Z_c u_1 = p_1 \tanh\,2\alpha L. \tag{37}$$

Using Eq. (13), u_1 can be written as a function of p_1, then the second equation of Eq. (37) leads to the following nonlinear equation for the unknown p_1:

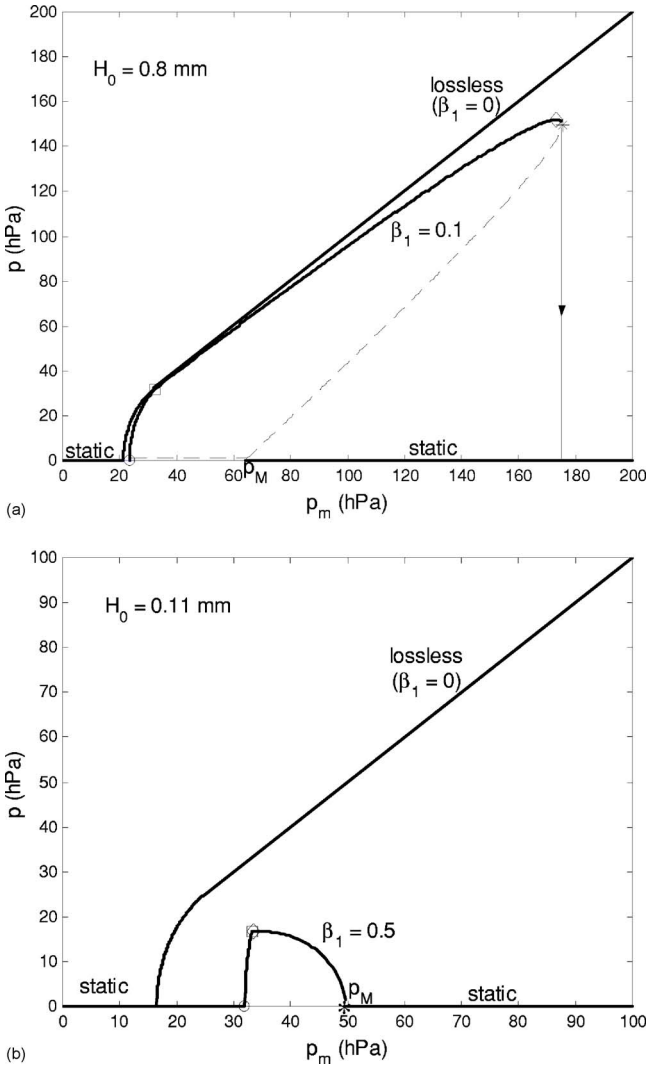

FIG. 4. Bifurcation's diagram: Pressure in the mouthpiece p vs mouthpressure p_m. Dotted line corresponds to an unstable branch and thick lines correspond to stable branches (including static solution). Losses correspond to a 50-cm-long cylindrical tube. The points corresponding to the different thresholds are labeled on the curve: (○) threshold of oscillation; (□) beating reed threshold; (◇) saturation threshold; (∗) extinction threshold. (a) Reed opening is $H_0 = 0.8$ mm ($p_M = KH_0 = 67$ hPa, $\beta_1 = 0.1$, and $\beta = 0.005 \ll 1$). (b) Reed opening is $H_0 = 0.11$ mm ($p_M = KH_0 = 50$ hPa, $\beta_1 = 0.5$, and $\beta = 0.001 \ll 1$).

$$-\beta_2 p_1 + (p_M - p_m + p_1)\sqrt{\frac{p_m - p_1}{p_M}} = 0. \tag{38}$$

From Eq. (38), p_1 can be calculated as a function of p_m. This leads to a third-order polynomial equation in $\Delta p_1 = p_m - p_1$ which can be solved by using, for example, Cardan's method. A detailed analysis, including the stability, is given in the Appendix. In the range of interest, for $\beta_2 < 1$ and $p_m > p_M$ there are two solutions, but only one is stable. In that case there is an inverse bifurcation scheme at extinction [Fig. 4(a)]. Above a threshold of extinction, written p_{me}, no solutions exist. For $\beta_2 \geqslant 1$ or $p_m < p_M$ only one solution exists, which is stable. In that case there is a direct bifurcation scheme at extinction [Fig. 4(b)].

As $\beta_2 \approx 2\beta_1$, it can be concluded that the parameter β_1, which has been shown previously to influence the threshold

of oscillations, is shown here to influence also the amplitude of the oscillations in the beating reed regime.

2. Nonbeating reed regime

By using Eq. (13), u_1 and u_2 can be written as functions of p_1 and p_2, respectively. Then Eq. (28) leads to a set of two nonlinear equations of the two unknowns $\Delta p_1 = p_m - p_1$ and $\Delta p_2 = p_m - p_2$:

$$2p_m - \Delta p_1 - \Delta p_2 = \beta[(p_M - \Delta p_1)\sqrt{\Delta p_1/p_M} + (p_M - \Delta p_2)\sqrt{\Delta p_2/p_M}],$$

$$(p_M - \Delta p_1)\sqrt{\Delta p_1/p_M} - (p_M - \Delta p_2)\sqrt{\Delta p_2/p_M} = \beta_1[\Delta p_2 - \Delta p_1]. \quad (39)$$

In the Appendix, it is shown that this system leads to the solving of a third-order polynomial equation, followed by a second-order one. Under the assumption that $\beta = 0$, i.e., $Z_0 = 0$, a great simplification occurs, the third order being reduced to a second order. Otherwise the threshold of existence of the solutions can be checked to be the same as the instability threshold for the static regime.

3. Bifurcation diagrams

To summarize, solving the set of equations (39) gives the nonbeating regimes, and solving Eq. (38) gives the beating regimes. This means that the bifurcation diagram can be completed. As an illustration, two typical bifurcation diagrams are displayed: one shows an inverse bifurcation at extinction [Fig. 4(a)] and the other one shows a direct bifurcation at extinction [Fig. 4(b)]. For the studied example, the parameter β is assumed to be small, this assumption being realistic for practical situations. The diagram of Fig. 4(a) is very similar to what can be observed with an artificial mouth (see, e.g., Dalmont *et al.*, 2000, or Atig *et al.*, 2004).

C. Thresholds from Raman's model

As displayed in Fig. 4(a), some remarkable points in the bifurcation diagrams can be brought out. These are:

(1) the threshold of oscillation $p_{m\mathrm{th}}$ for which oscillation starts when pressure increases slowly,
(2) the beating reed threshold $p_{m\mathrm{b}}$ for which the reed starts beating (for sake of simplicity, we omit here and in the following the precision "for the periodic regime of frequency $f = c/4L$," see explanations at the end of Sec. II C),
(3) the saturation threshold $p_{m\mathrm{s}}$ for which the maximum amplitude is reached,
(4) the extinction threshold $p_{m\mathrm{e}}$ beyond which there is no oscillation, and
(5) the inverse oscillation threshold $p_{m\mathrm{in}}$ for which oscillation starts when pressure decreases after the reed have been blocked on the lay.

In what follows the pressure values of these thresholds are calculated as a function of the parameters of the model, that is p_M, β, β_1, and β_2. The parameter β is usually small compared to unity. However, all the following results are general, it means that β is not supposed to be small compared to unity. On the contrary $\beta_2 \approx 2\beta_1$ and β_1 can be larger than unity, but, as discussed in the following, if $\beta_1 \geqslant 1$ no oscillation is possible. The conditions for an inverse or a direct bifurcation at the extinction are also derived.

1. Threshold of oscillation

This threshold is discussed in Sec. II B, Eq. (16).

2. Beating-reed threshold

The beating reed threshold is defined by the condition $\Delta p_2 = p_M$. Then at the beating threshold $p_2 = p_m - p_M$ is known, and p_1 is derived from Eq. (38):

$$p_1 = (p_m - p_M)\frac{(\tanh^2 \alpha L + 1)}{(\tanh^2 \alpha L - 1)} = (p_m - p_M)\frac{(\beta\beta_1 + 1)}{(\beta\beta_1 - 1)}. \quad (40)$$

Equation (39) remains valid, and yields to the particular value of the mouth pressure p_{mb} which is the beating reed threshold:

$$p_{m\mathrm{b}} = \left(\tfrac{1}{2} + \tfrac{1}{2}[\beta\beta_1 + \beta_1^2(1 - \beta\beta_1)]\right)p_M. \quad (41)$$

In the absence of losses $\beta = \beta_1 = 0$ and $p_{mb} = p_M/2$. If $\beta_1 = 1$ then $p_{m\mathrm{b}} = p_M$ and, as discussed in Sec. II B, no oscillation is possible, for any mouth pressure.

At the beating threshold, the two states p_{1b} and p_{2b} of the periodic regime are

$$p_{1\mathrm{b}} = \frac{\beta_1}{\beta_2}(1 - \beta_1^2)p_M,$$

$$p_{2\mathrm{b}} = -p_{1b} + \beta\beta_1(1 - \beta_1^2)p_M. \quad (42)$$

3. Saturation threshold

The saturation threshold is the point for which the amplitude of the oscillation is maximum, that is $\partial p_1/\partial p_m = 0$. This occurs when the maximum flow is reached ($u_1 = u_{\max} = 3\sqrt{3}/2u_A$), that is for $\Delta p_1 = p_M/3$ (see Fig. 3). Then, using $p_m = \Delta p_1 + p_1$ and $Z_c u_1 = p_1 \tanh(2\alpha L)$, Eq. (37) shows that

$$p_{ms} = \left(\frac{1}{3} + \frac{2}{3\sqrt{3}\beta_2}\right)p_M. \quad (43)$$

At this value, the corresponding pressures p_{1s} and p_{2s} are

$$p_{1\mathrm{s}} = \frac{2}{3\sqrt{3}\beta_2}p_M,$$

$$p_{2\mathrm{s}} = -p_{1\mathrm{s}} + \frac{2\beta}{3\sqrt{3}}p_M. \quad (44)$$

If β_2 tends to zero the saturation threshold as well as the amplitude of the oscillations tend to infinity. The saturation threshold cannot be lower than the beating reed threshold. Both thresholds are equal when $\beta_1 = 1/\sqrt{3}$. So the previous result is valid for $\beta_1 < 1/\sqrt{3}$. For $1 > \beta_1 > 1/\sqrt{3}$ the beating reed threshold is equal to the saturation threshold.

4. Extinction threshold

Due to losses, when the mouth pressure p_m is too large, there is no more oscillation. The maximum value for which oscillation is still possible is defined as the "extinction threshold." It is obtained from Eq. (38) which gives the beating reed periodic solutions. Two situations are possible. The first one is obtained for $\beta_2 < 1$. In that case the extinction threshold is larger than p_M and is given by

$$p_{me} = \left(\frac{1}{9} + \frac{2}{27\beta_2}(3+\beta_2^2)[\beta_2 + \sqrt{3+\beta_2^2}]\right)p_M. \tag{45}$$

Such a situation has been observed in experiments with an artificial mouth (Dalmont, 2000; Atig, 2004). The second situation is obtained for $\beta_2 > 1$, p_{me} is equal to p_M and in that case there is a direct bifurcation at extinction, thus p_{1e} and p_{2e} vanish.

5. Inverse oscillation threshold

The threshold $p_{\min}$ is the pressure for which oscillation starts when the pressure is decreased after the reed have been held motionless on the lay. It is equal to the lowest pressure for which the reed closes the reed-mouthpiece channel, that is $p_{min} = p_M$.

All the previous results about the thresholds are summarized in Fig. 5. It can be observed that all the threshold are different for $\beta_1 < 0.5$. For $\beta_2 = 1$, that is $\beta_1 \approx 0.5$, the extinction threshold reaches p_M, which means that the bifurcation becomes direct at extinction (p_M can be seen as the direct threshold of oscillation for decreasing a pressure). For $\beta_1 = 1/\sqrt{3}$ the saturation threshold reaches the beating reed threshold which means that the maximum amplitude is obtained at the beating reed threshold. Finally when $\beta_1 \geqslant 1$ all the thresholds collapse and no oscillation is possible.

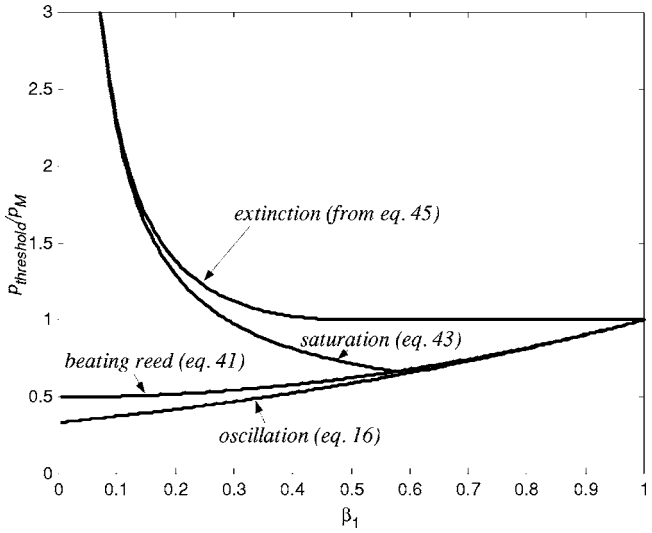

FIG. 5. Thresholds as a function of parameter β_1 with $\beta \ll 1$.

6. Instability threshold

The threshold of instability is discussed in the next section, because another dimensionless parameter needs to be introduced.

D. Stability analysis

As written at the end of Sec. III A, the periodic solutions are stable if the inequality (32) is true. The derivative of the function G defined in Eq. (29) is given by

$$G' = \frac{Z_c F' - \tanh \alpha L}{1 - Z_c F' \tanh \alpha L}. \tag{46}$$

According to Eq. (46), the stability function $G_{\text{stab}}(q)$ can be written as follows:

$$G_{\text{stab}}(q) = \frac{G'(q)+G'(-q)}{1+G'(q)G'(-q)} = \frac{\left(\frac{Z_c F'(p_1) - \tanh \alpha L}{1 - Z_c F'(p_1)\tanh \alpha L}\right) + \left(\frac{Z_c F'(p_2) - \tanh \alpha L}{1 - Z_c F'(p2)\tanh \alpha L}\right)}{1 + \left(\frac{Z_c F'(p_1) - \tanh \alpha L}{1 - Z_c F'(p_1)\tanh \alpha L}\right)\left(\frac{Z_c F'(p2) - \tanh \alpha L}{1 - Z_c F'(p2)\tanh \alpha L}\right)}, \tag{47}$$

or

$$G_{\text{stab}}(q) = \frac{Z_c F_{\text{stab}}(p_1,p_2) - \tanh 2\alpha L}{1 - Z_c F_{\text{stab}}(p_1,p_2)\tanh 2\alpha L} \tag{48}$$

with

$$F_{\text{stab}}(p_1,p_2) = \frac{F'(p_1)+F'(p_2)}{1+Z_c^2 F'(p_1)F'(p_2)}, \tag{49}$$

the stability condition being $G_{\text{stab}}(q) < 0$.

Because $\tanh 2\alpha L$ is positive, this condition can be split into two conditions:

$$F_{\text{stab}}(p_1,p_2) < Z_c^{-1} \tanh 2\alpha L,$$

$$F_{\text{stab}}(p_1,p_2) > Z_c^{-1} \coth 2\alpha L. \tag{50}$$

To check the stability of the periodic regimes the signs of the stability conditions (50) are first analyzed for the beating case and then for the nonbeating case. The details are given in the Appendix. For the beating case, $F'(p_2) = 0$ implies that $F_{\text{stab}}(p_1,p_2) = F'(p_1)$. For this case, it can be seen that the solutions p_1 corresponding to the upper branch of the bifurcation diagram are always stable, and the solutions corresponding to the lower branch are unstable, except for a very special case: a complete analysis could be done for the case, but it is without interest in practice, because it requires both large losses and large u_A.

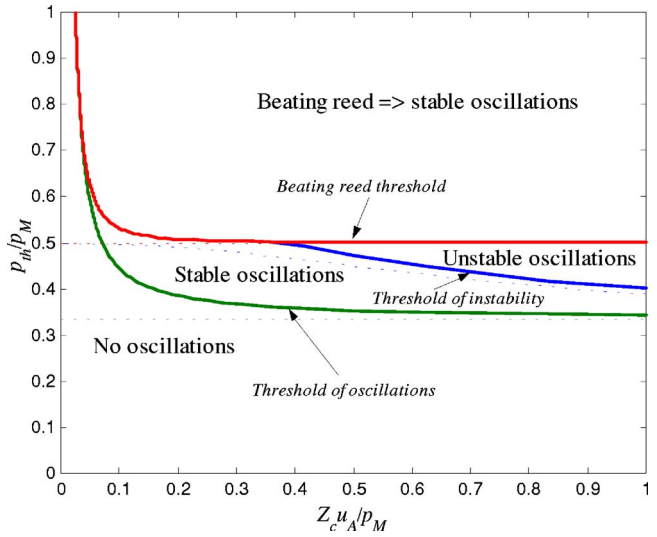

FIG. 6. (Color online) Thresholds as a function of the dimensionless flow amplitude of the nonlinear characteristics $\tilde{u}_A = Z_c u_A / p_M$. Dotted lines correspond to the lossless case. The instability region (for the fundamental regime) is between the threshold of instability and the beating reed threshold.

For the nonbeating reed ($p_{m\text{th}} < p_m < p_{m\text{b}}$), the analysis is not straightforward and the conclusion is not so simple. Nevertheless it can be checked that there is a low limit of the mouth pressure, called $p_{m\text{inst}}$, under which the oscillations are stable. If $p_{m\text{inst}} < p_m < p_{m\text{b}}$ oscillations are not stable and a period doubling can be observed as well as other regimes with larger periods, or even chaos (Kergomard *et al.*, 2004; Kergomard, 1995). The instability range is actually narrow because the beating reed threshold for the periodic regime of frequency $c/4L$ is in practice close to the threshold of instability. In the appendix the value of the threshold of instability is found for $\beta \ll 1$ [see Eq. (A32)]. This threshold is plotted in Fig. 6 as a function of $\tilde{u}_A = Z_c u_A / p_M$.

The threshold of instability increases significantly when losses increase and even disappears for some limit value of parameter $\tilde{u}_A$ depending on the value of the parameter β_1. This result confirms numerical, *ab initio* calculations given in Ollivier *et al.* (2004). The limit value of β_1 up to which there is no instability range is found to be at the second order of $\tilde{u}_A = Z_c u_A / p_M$:

$$\tanh \alpha L = \tfrac{1}{2}\tilde{u}_A^3[1 - \tilde{u}_A^2] \quad \text{for } \beta \ll 1 \tag{51}$$

This limit value is rather low, which means that period doubling might usually not be observed. Indeed, with standard values of the limit pressure $p_M = 10$ kPa and maximum flow $u_{\max} = 4.10^{-4}$ m^3/s, $\tilde{u}_A$ is found to be $\tilde{u}_A = 0.22$. This leads to $\beta_{1\text{inst}} = 0.023$, which is much lower than the actual value $\beta_1 = 0.11$ for a 16-mm-diam pipe of length 0.5 m. This means that no period doubling may be observed. However with a reed of low stiffness (a weak reed), and a rather loose embouchure the value of β_1 is decreased while the value of $\beta_{1\text{inst}}$ is increased. So, it is theoretically possible to obtain period doubling as noted by Kergomard (1995) with some unusual embouchure.

IV. DISCUSSION

Based upon a simplified model of the clarinet, solutions for the mouthpiece pressure and their stability have been found analytically. The playing range of the clarinet is found to depend on two parameters. The first one is the minimum pressure p_M sufficient to close the reed channel in static regime. The second parameter $\beta_1 = Y p_M / u_A$ is the ratio of the input admittance of the pipe at the playing frequency to the flow amplitude parameter of the nonlinear characteristic u_A divided by p_M. The definition of this second parameter β_1 shows that the playing range depends on the balance between the embouchure, characterized by its nonlinear characteristics, and the pipe characterized by its input admittance. In an extreme situation, if, for example, the reed channel cross section is small compared to the pipe cross section, no oscillation for any mouth pressure occurs. Such an extreme situation can also be reached if losses are too large. This is the case if side holes are too small since in that case nonlinear losses become large (Keefe, 1983; Dalmont *et al.*, 2001a). Parameter β_1 also determines the bifurcation scheme at extinction. If the parameter β_1 is lower than 0.5 the bifurcation is inverse at the extinction and the extinction threshold is larger than p_M, showing an hysteretic phenomenon at extinction [see Atig *et al.* (2004) for experimental evidence]. This is probably the most usual situation. On the contrary if the parameter β_1 is larger than 0.5 the bifurcation is direct at the extinction and the extinction threshold is equal to p_M. These same two parameters also determine the threshold of oscillation (Kergomard *et al.*, 2000) as well as the beating reed threshold for the periodic regime of frequency $c/4L$. However, the stability of the oscillations also depends on another parameter: the dimensionless volume velocity amplitude $\tilde{u}_A = Z_c u_A / p_M$ of the nonlinear characteristics. This parameter also expresses the balance between the embouchure and the pipe and its role has been first emphasized by Wilson and Beavers (1974) and Kergomard (1995) in the context of the lossless model. A limit value of β_1, as a function of $\tilde{u}_A$, exists up to which oscillations at the fundamental frequency are always stable. For realistic values of the physical parameters, β_1 is shown to be larger than this limit value. This might explain why period doubling is not usually observed on a standard clarinet.

V. CONCLUSION

All these results are in a good agreement with experimental observations (Atig *et al.*, 2004) showing that, despite its simplicity, Raman's model is a powerful tool for the study of the clarinet. The present results give a new enlightenment on the playing of the clarinet. In particular, it reveals the possibility of playing pianissimo by playing near the threshold of extinction when the bifurcation at extinction is direct. The way clarinet players use this possibility in performing is a subject for further investigations.

ACKNOWLEDGMENTS

We acknowledge Aude Lizée for discussions about the beating reed threshold, the clarinetist Pierre-André Taillard

for discussions on the musical consequences of our calculations, and Kees Nederveen for a careful and enlightened reading of the paper.

APPENDIX: STUDY OF THE OSCILLATING SOLUTIONS AND THEIR STABILITY

The Appendix gives the detailed calculation of the oscillating solutions and their stability. In order to simplify the presentation, dimensionless quantities are used. Pressures are divided by the limit pressure p_M and flows are multiplied by the ratio Z_c/p_M, where Z_c is the characteristic impedance of the tube.

Starting from Eq. (13), it means that the following nonlinear function $u=F(p)$ is considered:

$$u = u_A(1-\Delta p)\sqrt{\Delta p} \quad \text{if } \Delta p \leqslant 1$$

$$u = 0 \quad \text{if } \Delta p \geqslant 1, \tag{A1}$$

where $\Delta_p = p_m - p$, and $u_A = \sqrt{2} Z_c w H / \sqrt{\rho p_M}$. Note that in Kergomard (1995) p_m and u_A are denoted γ and ζ, respectively. The two cases of the beating reed and the nonbeating reed are studied successively.

1. Beating case

For one of the solutions, p_2, $F(p)=0$. The other solution, p_1, is found to be solution of Eq. (37), rewritten as follows:

$$H(X) = \frac{1}{\beta_2}(1-X^2)X + X^2 - p_m = 0, \tag{A2}$$

where $X = \sqrt{\Delta p_1} = \sqrt{p_m - p_1}$, which satisfies $0 < X < 1$.

The first condition of stability from Eq. (50) is first examined. If it is satisfied, the solution is stable, if not, the second condition remains to be examined. Because $F(p_2)$ is zero as well as its derivative, the condition is

$$F'(p) < \tanh 2\alpha L \quad \text{at } p = p_1. \tag{A3}$$

Using Eq. (37), we notice that

$$F(p_1) = [H(X) + p_1]\tanh 2\alpha L, \tag{A4}$$

which leads to the following stability condition:

$$H'(X) > 0$$

with

$$H(X) = 0. \tag{A5}$$

The derivative $H'(X)$ of $H(X)$ with respect to X is given by

$$H'(X) = (1-3X^2)/\beta_2 + 2X. \tag{A6}$$

For $X=0$, $H(X)=-p_m$ and $H'(X)=1/\beta_2$. For $X=1$, $H(X)=1-p_m$ and $H'(X)=2(1-1/\beta_2)$. The derivative of $H(X)$ vanishes for a unique, positive value

$$X_e = \tfrac{1}{3}[\beta_2 + \sqrt{\beta_2^2 + 3}]. \tag{A7}$$

Because $H'(X)$ is a second-order polynomial, above this value X_e, $H'(X)$ is negative, below, it is positive. If $\beta_2 < 1$, $X_e < 1$. On the contrary, if $\beta_2 > 1$, $X_e > 1$. We now distinguish the two cases:

a. First case: $\beta_2 > 1$

Function $H(X)$ increases from $-p_m$ for $X=0$ to $1-p_m$ when $X=1$.

If $p_m > 1$, there are no solutions. If $p_m < 1$, there is a unique solution, with a positive derivative, therefore the solution is stable.

b. Second case: $\beta_2 < 1$

Function $H(X)$ increases from $-p_m$ for $X=0$, then goes through a maximum value at $X=X_e$, and finally decreases to $1-p_m$ when $X=1$.

If $p_m < 1$, there is a unique solution $X < X_e$ with a positive derivative, thus the solution is stable.

If $p_m > 1$, there are no solutions if $H(X_e) < 0$, and two solutions if $H(X_e) > 0$. This condition can be written as $H(X_e) = \text{function}(\beta_2) - p_m > 0$. Therefore there are two solutions if

$$p_m < \frac{1}{\beta_2}(1-X_e^2)X_e + X_e^2 = \frac{1}{9} + \frac{2}{27\beta_2}(3+\beta_2^2) \times [\beta_2 + \sqrt{\beta_2^2+3}] = p_{me}. \tag{A8}$$

The value p_{me} is interpreted as the extinction threshold. The solution satisfying $X < X_e$ has a positive derivative: it means that the solution such as $p_1 > p_{me}$, on the upper branch in Fig. 4, is stable. The other solution, satisfying $X > X_e$, corresponding to the lower branch, has a negative derivative. It is expected to be unstable, the condition being that the second condition from Eq. (50) is not fulfilled, i.e.,

$$F'(p_1) < \coth 2\alpha L. \tag{A9}$$

Using Eq. (A4), this condition is rewritten as

$$\left[-\frac{1}{2X}H'(X) + 1\right] < \coth^2 2\alpha L,$$

or

$$\frac{1-3X^2}{2X} > -\frac{1}{u_A}\coth 2\alpha L. \tag{A10}$$

The function of the left-side member is decreasing from $X=X_e$ to $X=1$. Thus a sufficient condition is that the condition is satisfied for $X=1$. A final sufficient condition is found to be

$$u_A \tanh 2\alpha L < 1. \tag{A11}$$

We notice that for $p_m=1$, the two solutions are $X=\beta$ and $X=1$: thus the condition is also necessary. As a conclusion, for given values of u_A and α, the condition for the instability of the lower branch solution for every value of p_m lying in the interval $[1, p_{me}]$ is given by inequality (A11). This condition is satisfied for every practical case, but we notice that it is possible to have $\beta = u_A \tanh \alpha L < 1$ while $u_A \tanh 2\alpha L > 1$. As a matter of fact, this would imply a large value of

either the losses (αL) or the parameter u_A (at least u_A larger than unity), and this case is probably not encountered in practice.

2. Nonbeating case

a. Existence of the solutions

The solutions p_1 and p_2 are given by Eq. (39)

$$2p_m - \Delta p_1 - \Delta p_2 = \beta[(1-\Delta p_1)\sqrt{\Delta p_1} + (1-\Delta p_2)\sqrt{\Delta p_2}] \tag{A12}$$

$$(1-\Delta p_1)\sqrt{\Delta p_1} - (1-\Delta p_2)\sqrt{\Delta p_2} = \beta_1(\Delta p_2 - \Delta p_1), \tag{A13}$$

where $\Delta p_1 = p_m - p_1$ and $\Delta p_2 = p_m - p_2$.

Writing

$$\Sigma = \sqrt{\Delta p_1} + \sqrt{\Delta p_2}, \quad \Pi = \sqrt{\Delta p_1}\sqrt{\Delta p_2}, \tag{A14}$$

the first equation leads to

$$2p_m - \Sigma^2 + 2\Pi = \beta\Sigma(1 - \Sigma^2 + 3\Pi) \tag{A15}$$

and the second one, after elimination of $\sqrt{\Delta p_1} = \sqrt{\Delta p_2}$, corresponding to the static regime,

$$1 - \Sigma^2 + \Pi = -\beta_1\Sigma. \tag{A16}$$

Eliminating Π, Σ is found to be solution of the following equation of the third order:

$$2\beta\Sigma^3 - (1 + 3\beta\beta_1)\Sigma^2 + 2(\beta_1 - \beta)\Sigma + 2(1 - p_m) = 0. \tag{A17}$$

The solution is particularly easy to find if parameter β is small, and assumed to be zero.

The threshold of existence for the solutions is given by $\Sigma^2 = 4\Pi$. Using Eqs. (A15) and (A16), we get

$$p_m = \beta(1-\Pi)\sqrt{\Pi} + \Pi \tag{A18}$$

and

$$3\Pi - 2\beta_1\sqrt{\Pi} - 1 = 0. \tag{A19}$$

Eliminating Π, the threshold is found be equal to the threshold of instability of the static regime.

b. Stability of the solutions

In order to be stable, the solutions need to satisfy one of equations (50). After some algebra, they are found to be

$$\text{either } K < 1 \tag{A20}$$

$$\text{or } K > \coth^2 2\alpha L, \tag{A21}$$

where

$$K = \frac{2\Sigma(3\Pi - 1)}{\beta_2[4\Pi + u_A^2[(1+3\Pi)^2 - 3\Sigma^2]]}. \tag{A22}$$

Using Eq. (A19), quantity K is found to be equal to unity at the threshold of existence. Then, a numerical analysis shows that, for increasing p_m, the factor $(3\Pi - 1)$ becomes negative, and the condition (A20) is fulfilled. Then the denominator vanishes, the quantity K tending to $-\infty$, then decreases from $+\infty$. Therefore the instability threshold appears to be given by the single condition (A21), written as follows:

$$4\Pi + u_A^2[(1+3\Pi)^2 - 3\Sigma^2] = \frac{2\Sigma(3\Pi - 1)}{\beta_2 \coth^2 2\alpha} \tag{A23}$$

or

$$\frac{4\Pi}{u_A^2} + (1+3\Pi)^2 - 3\Sigma^2 = \frac{\beta_1}{1+\beta\beta_1}\Sigma(3\Pi - 1). \tag{A24}$$

An analytical solution is difficult to find, except if $\beta = u_A \tanh\alpha$ is small. With this assumption, the following equation needs to be solved:

$$\frac{4\Pi}{u_A^2} + (1+3\Pi)^2 - 3\Sigma^2 = \beta_1\Sigma(3\Pi - 1), \tag{A25}$$

where

$$2p_m - \Sigma^2 + 2\Pi = 0 \tag{A26}$$

and

$$1 - \Sigma^2 + \Pi = -\beta_1\Sigma. \tag{A27}$$

This leads to a fourth-order polynomial equation in Π, thus we limit the analytical calculation to a first-order approximation with respect to parameter β_1. The following result is obtained:

$$\Sigma^2 = 1 + \Pi + \beta_1\sqrt{1+\Pi}.$$

Then, using Eq. (A25):

$$9\Pi^2 + \left[\frac{4}{u_A^2} + 3\right]\Pi - 2 = \beta_1\sqrt{1+\Pi}(2+3\Pi). \tag{A28}$$

At the zeroth order of β_1 (no losses are present), the result corresponding to Eq. (45) of the Kergomard (1995) is obtained:

$$\Pi_0 = \frac{1}{18}\left[-\frac{4}{u_A^2} - 3 + \sqrt{\left[\frac{4}{u_A^2} + 3\right]^2 + 72}\right], \tag{A29}$$

then at the first order

$$\Pi = \Pi_0 + \frac{\beta_1\sqrt{1+\Pi_0}(2+3\Pi_0)}{18\Pi_0 + 3 + 4/u_A^2} \tag{A30}$$

and finally the threshold of instability is found to be

$$p_{m,\text{inst}} = \tfrac{1}{2}[1 - \Pi + \beta_1\sqrt{1+\Pi_0}]. \tag{A31}$$

This result has been found to be in good agreement with numerical simulation, which shows that the bifurcation corresponds to a period doubling (it is deduced that the threshold of instability increases significantly when losses increase).

An interesting point is that this threshold can reach the beating threshold when losses become larger, and the insta-

bility range disappears, as we will prove now. At the beating threshold, $\Pi=\beta_1$ and $\Sigma=1+\beta_1$, thus the equality of the thresholds is given by Eq. (A24):

$$\frac{4\beta_1}{u_A^2}+6\beta_1-2=\frac{-\beta_1}{1+\beta_1\beta}(1+\beta_1)(1-3\beta_1). \tag{A32}$$

This leads to a third-order polynomial equation:

$$3\beta_1^3u_A^2(u_A^2-2)+\beta_1^2u_A^2+\beta_1(2+2u_A^2-u_A^4)-u_A^2=0. \tag{A33}$$

For small u_A, a series expansion leads to

$$\beta_1=\frac{u_A^2}{2}\left[1-u_A^2+\frac{5}{4}u_A^4-\frac{1}{2}u_A^6\right]. \tag{A34}$$

For losses larger than this value, no period doubling occurs. For practical cases; the second order in the bracket is certainly sufficient.

Atig, M., Dalmont, J.-P., and Gilbert, J. (**2004**). "Saturation mechanism in clarinet-like instruments, the effect of the localized non-linear losses," Appl. Acoust. **65**, 1133–1154.

Dalmont, J.-P., Ducasse, E., and Ollivier, S. (**2002**). "Saturation mechanism in reed instruments," Proceedings of the Third EEA European Congress on Acoustic, Sevilla, Spain.

Dalmont, J.-P., Ducasse, E., and Ollivier, S. (**2001a**). "Practical consequences of tone holes nonlinear behaviour," International Symposium of Musical Acoustics, Perugia, pp. 153–156.

Dalmont, J.-P., Gilbert, J., and Kergomard, J. (**2000**). "Reed instruments, from small to large amplitude periodic oscillations and the Helmholtz motion analogy," Acust. Acta Acust. 86, 671–684.

Dalmont, J.-P., Gilbert, J., and Ollivier, S. (**2003**). "Non-linear characteristics of single reed instruments: Quasi-static volume flow and reed opening measurements," J. Acoust. Soc. Am. **114**, 2253–2263.

Dalmont, J.-P., and Kergomard, J. (**1995**). "Elementary model and experiments for the Helmholtz motion of single reed wind instruments," Proceedings of the International Symposium on Musical Acoustics, Dourdan, France, pp. 114–120.

Dalmont, J.-P., Nederveen, K., and Joly, N. (**2001b**). "Radiation impedance of tubes with different flanges: Numerical and experimental investigations," J. Sound Vib. **244**, 505–534.

Fletcher, N. H., and Rossing, T. D. (**1998**). *The Physics of Musical Instruments* (Springer, New York).

Friedlander, F. G. (**1953**). "On the oscillations of a bowed string," Proc. Cambridge Philos. Soc. **49**, 516–530.

Grand, N., Gilbert, J., and Laloé, F. (**1997**). "Oscillation threshold of woodwinds instruments," Acustica **1**, 137–151.

Hirschberg, A. (**1995**). "Aero-acoustics of wind instruments," in *Mechanics of Musical Instruments*, edited by A. Hirschberg, J. Kergomard, and G. Weinreich, CISM Courses and Lectures No. 355 (Springer, Wien).

Keefe, D. H. (**1983**). "Acoustic streaming, dimensional analysis of nonlinearities, and tone hole mutual interactions in woodwinds," J. Acoust. Soc. Am. **73**, 1804–1820.

Keller, J. B. (**1953**). "Bowing of violin strings," Commun. Pure Appl. Math. **6**, 483–493.

Kergomard, J. (**1995**). "Elementary considerations on red-instruments oscillations," in *Mechanics of Musical Instruments*, edited by A. Hirschberg, J. Kergomard, and G. Weinreich, CISM Courses and Lectures No. 355 (Springer, Wien).

Kergomard, J., Dalmont, J.-P., Gilbert, J., and Guillemain, P. (**2004**). "Period doubling on cylindrical reed instruments," 7ème Congrès Français d'Acoustique, Strasbourg, pp. 113–114.

Kergomard, J., Ollivier, S., and Gilbert, J. (**2000**). "Calculation of the spectrum of self-sustained oscillators using a variable truncation method," Acust. Acta Acust. 86, 685–703.

Maganza, C., Caussé, R., and Laloé, F. (**1986**). "Bifurcations, period doublings and chaos in clarinet like systems," Electron. Lett. **1**, 295–302.

Mc Intyre, M. E., Schumacher, R. T., and Woodhouse, J. (**1983**). "On the oscillations of musical instruments," J. Acoust. Soc. Am. **74**, 1325–1345.

Nederveen, C. J. (**1998**). *Acoustical Aspects of Woodwind Instruments* (Northern Illinois University Press, DeKalb).

Norris, A. N., and Sheng, I. C. (**1989**). "Acoustic radiation from a circular pipe with an infinite flange," J. Sound Vib. **135**, 85–93.

Ollivier, S., Dalmont, J.-P., and Kergomard, J. (**2004**). "Idealized models of reed woodwinds. I. Analogy with the bowed string," Acust. Acta Acust. 90, 1192–1203.

Ollivier, S., Kergomard, J., and Dalmont, J.-P. (**2005**). "Idealized models of reed woodwinds. II. On the stability of 'two step' oscillations," Acust. Acta Acust. 91, 166–179.

Polack, J.-D., Meynial, X., Kergomard, J., Cosnard, C., and Bruneau, M. (**1987**). "Reflection function of a plane wave in a cylindrical tube," Rev. Phys. Appl. **22**, 331–339.

Raman, C. V. (**1918**). "On the mechanical theory of vibrations of bowed strings," Indian Assoc. Cult. Sci. Bull., **15**(1), 1-158

Schelleng, J. C. (**1973**). "The bowed string and the player," J. Acoust. Soc. Am. **53**, 26-41

Wilson, T. A., and Beavers, G. S. (**1974**). "Operating modes of the clarinet," J. Acoust. Soc. Am. **56**, 653–658.

Woodhouse, J. (**1993**). "Idealized models of a bowed string," Acustica **79**, 233–250.